Influence of the Protein Environment on the Properties of a Tyrosyl Radical in Reaction Centers from *Rhodobacter sphaeroides*†

A. J. Narváez,‡ L. Kálmán,‡,§ R. LoBrutto,|| J. P. Allen,*,‡ and J. C. Williams‡

Departments of Chemistry and Biochemistry and of Plant Biology, Arizona State University, Tempe, Arizona 85287

Received July 15, 2002; Revised Manuscript Received October 12, 2002

ABSTRACT: The influence of the local environment on the formation of a tyrosyl radical was investigated in modified photosynthetic reaction centers from *Rhodobacter sphaeroides*. The reaction centers contain a tyrosine residue placed ∼10 Å from a highly oxidizing bacteriochlorophyll dimer. Measurements by both optical and electron paramagnetic resonance spectroscopy revealed spectral features that are assigned as arising primarily from an oxidized bacteriochlorophyll dimer at low pH values and from a tyrosyl radical at high pH values, with a well-defined transition that occurred with a pK_a of 6.9. A model based on the wild-type structure indicated that the Tyr at M164 is likely to form a hydrogen bond with His M193 and to interact weakly with Glu M173. Substitution of Tyr or Glu for His at M193 increased the pK_a for the transition from 6.9 to 8.9, while substitution of Gln for His M193 resulted in a higher pK_a value. Substitution of Glu M173 with Gln resulted in loss of the partial formation of the tyrosyl that occurs in the other mutants at low pH values. The results are interpreted in terms of the ability of the residues to act as proton acceptors for the oxidized tyrosine, with the pK_a values reflecting those of either the putative proton acceptor or the tyrosine, in accord with general models of amino acid radicals.

In *Rhodobacter sphaeroides*, light energy is transformed into chemical energy in a series of coupled electron and proton-transfer processes, with the primary photochemical process occurring in the reaction center, a membrane-bound pigment−protein complex. The reaction center contains three protein subunits, called the L, M, and H subunits, with the L and M subunits forming a structure with an approximate 2-fold symmetry that encases the cofactors (see refs *1* and *2* for reviews). Photoexcitation of a bacteriochlorophyll dimer leads to electron transfer, resulting in an oxidized dimer and a reduced quinone acceptor. An exogenous water-soluble cytochrome c_2 reduces the oxidized dimer, and a second excitation produces another electron transfer to the secondary quinone, which then leaves the reaction center carrying both the electrons and associated protons.

Since the discovery of a tyrosine radical in ribonucleotide reductase (*3*), stable and transient tyrosine radicals have been identified in mammalian prostaglandin H synthase, photosystem II, galactose oxidase, and cytochrome oxidase (see ref *4* for a review). We have reported a modified *Rb. sphaeroides* reaction center capable of generating a tyrosine radical (*5*). The ability to generate light-induced amino acid radicals in the well-characterized reaction center provides a means of investigating the involvement of these protein radicals in enzymatic reactions. In particular, the specific role of the protein environment in establishing the functional properties of amino acid radicals generated in this model system is investigated in this study. Another artificial tyrosyl radical containing system has been engineered by Gray and co-workers (*6*). In this complementary system, azurin modified with a rhenium complex yields a high-potential oxidant that can produce either tyrosyl or tryptophan radicals during light-induced irreversible oxidation of the protein. The properties of highly reactive radicals can be probed by kinetic and structural analyses of these modified protein systems.

The reaction center that is capable of tyrosine oxidation is modified in a key property of the bacteriochlorophyll dimer, the oxidation/reduction midpoint potential. The midpoint potential has been found to be specifically dependent upon the number of hydrogen bonds between the conjugated carbonyl groups of the dimer and the surrounding protein environment (*7*). By altering the protein so that the dimer has a maximal number of such hydrogen bonds, with an additional mutation of a nearby tyrosine, the midpoint potential was raised sufficiently for the dimer to be capable of oxidation of tyrosine residues (*6*). The highly oxidizing reaction center was formed by combining four different amino acid substitutions, Leu L131 to His, Leu M160 to His, Phe M197 to His, and Tyr M210 to Trp. A tyrosine residue introduced into these modified reaction centers at Arg M164, which is located approximately 10 Å from the edge of the dimer, resulted in a strain designated the Y_M mutant [LH(L131) + LH(M160) + RY(M164) + FH(M197) + YW(M210)]. In these reaction centers, after light excitation leads to the transfer of an electron from the donor to the primary quinone, the tyrosine forms a radical by electron transfer to the oxidized dimer. The pH dependence of this reaction was interpreted as being due to the ability of nearby residues to serve as proton acceptors, resulting in a neutral tyrosyl radical.

† This work was supported by Grant 1999-01753 from the USDA and by Grant MCB 0131764 from the NSF.

* To whom correspondence should be addressed: Phone 480-965-8241; fax 480-965-2747; e-mail jallen@asu.edu.

‡ Department of Chemistry and Biochemistry.

§ Permanent address: Department of Biophysics, University of Szeged, H-6722, Szeged, Egyetem u. 2, Hungary.

|| Department of Plant Biology.

10.1021/bi0264566 CCC: $22.00
Published on Web 11/23/2002

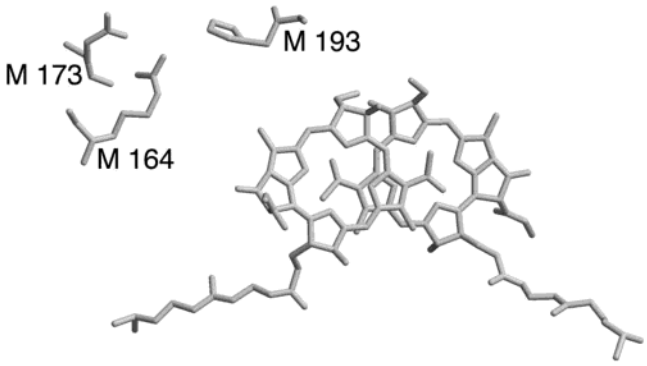

FIGURE 1: View of the bacteriochlorophyll dimer and nearby amino acid residues Arg M164, Glu M173, and His M193 in the wild-type reaction center from *Rb. sphaeroides*. Arg M164 is located approximately 10 Å from the edge of the bacteriochlorophyll dimer and approximately 3 Å from both His M193 and Glu M173. In this view the 2-fold symmetry axis of the protein is aligned vertically, and the periplasmic surface is at the top of the figure. The substitution Arg to Tyr at M164 was made in the Y_M mutants.

To understand how the environment influences the properties of the tyrosine at M164, we have replaced two residues, His M193 and Glu M173, that are modeled to be within hydrogen-bonding distance of the phenolic proton of the tyrosine (Figure 1). His M193 was replaced with three other residues, Tyr in the Y_M + HY(M193) mutant, Glu in the Y_M + HE(M193) mutant, and Gln in the Y_M + HQ(M193) mutant. These three substitutions have comparable sizes to His, but Tyr and Glu should have significantly altered proton-accepting characteristics, and Gln cannot serve as a proton acceptor. Another substitution, the exchange of Gln for Glu at M173, in the Y_M + EQ(M173) mutant results in replacement with an amino acid residue that is of essentially the same size but is unable to serve as a proton acceptor. The formation of the tyrosyl radical in these mutants compared to the Y_M mutant was probed by optical and electron paramagnetic resonance (EPR)[1] spectroscopy. Of particular interest was the determination of the pH dependence of the radical formation, since shifts in this dependence should be indicative of changes in the residues involved in proton transfer.

MATERIALS AND METHODS

Construction of Mutants and Protein Isolation. Sextuple mutants of reaction centers from *Rb. sphaeroides* were constructed by oligonucleotide-directed mutagenesis and by cloning of restriction fragments as previously described (*7*). Cells were grown semiaerobically, and reaction centers were isolated from all strains as previously described (*8*) except that 0.05% Triton X-100 was used as the detergent in the chromatography step. After isolation, the reaction centers were maintained in 15 mM Tris-HCl, pH 8.0, 0.05% Triton X-100, and 1 mM ethylenediaminetetraacetic acid. For measurements at other pH values, the samples were either dialyzed against a buffer at the appropriate pH, or for small increments, adjustments were made with 100 mM NaOH or 100 mM HCl. For the EPR spectroscopy, samples were concentrated by use of a Centricon microconcentrator (Amicon).

Optical and EPR Spectroscopy. The optical spectra of isolated reaction centers were obtained on a Cary 5 spectrophotometer (Varian). Illumination of the samples was achieved by employing an Oriel tungsten lamp with an 870 nm filter at low light levels that resulted in fully reversible spectral changes. For the optical spectra, the reaction centers were at a concentration of 1.5 μM in 15 mM Tris-HCl buffer, 0.05% Triton X-100, 100 mM NaCl, and 100 μM terbutryn. The spectral changes were measured in two regions: the near-infrared region (700−1000 nm) to monitor absorption changes in the dimer band and the 400−500 nm region to monitor absorption changes in the tyrosine signal. Measurements were performed at room temperature.

The EPR measurements were performed on a Bruker E580 X-band spectrometer with a protein concentration of 250 μM in 15 mM Tris-HCl, 0.05% Triton X-100, and 1 mM terbutryn. Experiments were performed at room temperature with a field modulation of 100 kHz, an amplitude of 0.4 mT, a microwave power of 10 mW, and a microwave frequency of 9.64 GHz. The reported *g* values include corrections for small frequency differences in the measurements. The spectra were obtained by first averaging 100 scans while the samples were illuminated in the cavity with a 1000 W Oriel tungsten lamp and then subtracting the average of 100 scans that were recorded while the samples were in the dark. Illumination was achieved with low light levels with a 10 cm water filter coupled to a 1.2 m long and 1 cm diameter fiber optic. Samples were illuminated in intervals of 8 s in the light and 8 s in the dark. These intervals were sustained throughout the duration of 100 scans for each spectrum. Spin quantitation was determined by use of the program Xepr (Bruker).

RESULTS

Optical Spectra. In the near-infrared region, wild-type reaction centers have absorption bands at 865 nm from the bacteriochlorophyll dimer, at 800 nm from the bacteriochlorophyll monomers, and at 765 nm from the bacteriopheophytins. In the presence of light, the spectra of wild-type reaction centers show an absorption decrease at 865 nm and an electrochromic shift of the bacteriochlorophyll monomer bands around 800 nm due to the oxidation of the dimer, and an electrochromic shift of the bacteriopheophytin band near 760 nm due to reduction of the quinone.

All of the mutants showed pH-dependent spectral features, which were similar to each other but differed from the wild-type pattern as has been previously observed for the Y_M mutant (*6*). For example, at low pH values, the mutant Y_M + HY(M193) showed spectral features that were nearly identical to those of wild type (Figure 2A). At high pH the spectral features are notably changed for the mutant. The lack of both the bleaching at 865 nm and the bandshift at 800 nm indicates that the dimer is not oxidized under these conditions. The electrochromic shift at 760 nm is still observed, indicating the presence of the reduced quinone.

In the 400−500 nm region, the light-minus-dark spectra of wild-type reaction centers show a broad band centered near 430 nm. In contrast, the light-minus-dark difference spectra of the Y_M mutants exhibit a new feature, an absorption decrease at 420 nm that became larger as the pH was increased. In the resulting spectra of, for example, the Y_M + HY(M193) mutant, a small absorption increase centered near 450 nm and an absorption decrease at 420 nm was observed (Figure 2B).

[1] Abbreviation: EPR, electron paramagnetic resonance.

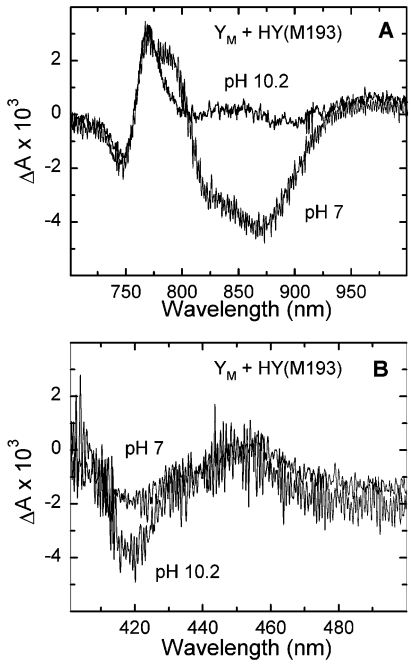

FIGURE 2: Light-minus-dark difference optical spectra for reaction centers from the Y_M + HY(M193) mutant at different pH values. Optical difference spectra are shown at pH 7.0 and pH 10.2 in (A) the near-infrared region and (B) the 400−500 nm region. The concentration of the samples for all spectra was 1.5 μM. Illumination was performed with a 1000 W Oriel tungsten lamp with an 870 nm interference filter.

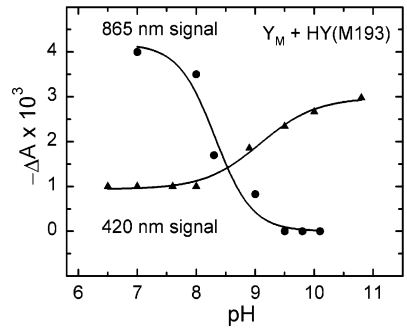

FIGURE 3: Correlation of the light-minus-dark absorption differences at 420 nm (▲) and 865 nm (●) for reaction centers from the Y_M + HY(M193) mutant at different pH values. The data shown include a baseline correction for nonzero absorption at 500 nm (Figure 2). The lines are fits to the Henderson−Hasselbalch equation, with pK_a values of 8.9 ± 0.1 and 8.7 ± 0.1 for the 420 and 865 nm data, respectively.

The increase in the negative absorption at 420 nm with increasing pH matches the loss of the bleaching at 865 nm in light-minus-dark optical spectra. For the Y_M + HY(M193) mutant, both pH dependencies can be fitted to a titration curve, yielding pK_a values of 8.9 for the 420 nm signal and 8.7 for the 865 nm signal, with estimated errors of ±0.1 (Figure 3). This correlation demonstrates that the loss of the oxidized dimer is associated with the gain of another state that causes the absorption decrease at 420 nm. The extent of the changes in the optical spectra with pH differed for each mutant (Figure 4). A pK_a value associated with the absorption changes was determined for each mutant, although a full titration was out of the range that could be obtained for the Y_M + HQ(M193) mutant.

EPR Spectra. Room-temperature light-minus-dark difference EPR spectra at pH 9 of all the mutants showed a similar

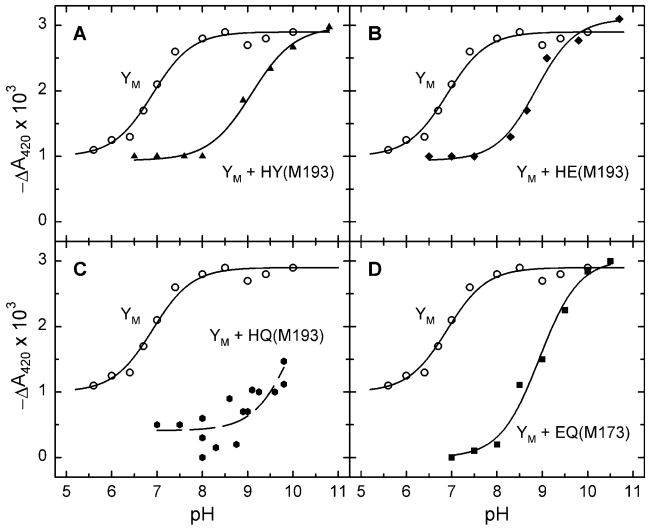

FIGURE 4: Effect of mutations on the pH dependence of the absorption changes at 420 nm for reaction centers from (A) the Y_M + HY(M193) mutant (▲), (B) the Y_M + HE(M193) mutant (◆), (C) the Y_M + HQ(M193) mutant (⬢), and (D) the Y_M + EQ(M173) mutant (■), compared to the Y_M mutant (○). The lines are fits to the Henderson−Hasselbalch equation, with pK_a values of 6.9, 8.9, 8.9, and 8.9 for the Y_M, Y_M + HY(M193), Y_M + HE(M193), and Y_M + EQ(M173) mutants, respectively, with an estimated error of ±0.1. The fit of the data for the Y_M + HQ(M193) mutant was constrained to have a maximal value of 0.003 at high pH and yielded a pK_a of approximately 10.

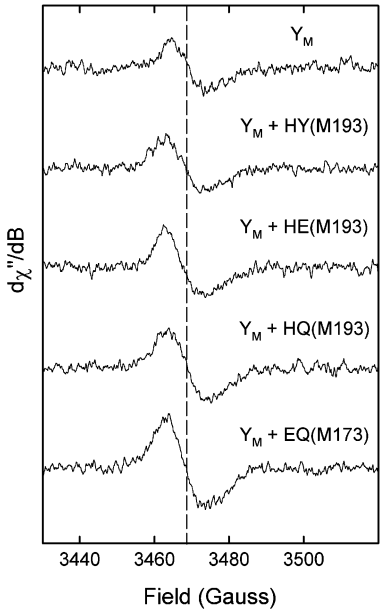

FIGURE 5: Light-minus-dark difference X-band EPR spectra of mutant reaction centers at pH 9. The spectra have *g* values of 2.0042, 2.0042, 2.0043, 2.0042, and 2.0043, with an estimated error of ±0.0005, and widths of 10, 10, 11, 10, and 11 G for the Y_M, Y_M + HY(M193), Y_M + HE(M193), Y_M + HQ(M193), and Y_M + EQ(M173) mutants, respectively. The vertical dashed line shows the position of $g = 2.0042$.

single-derivative shape with a calculated *g* value centered at 2.0042 ± 0.0005 (Figure 5). Widths of all these signals were calculated to be approximately 10 G. These spectra are clearly different from that of wild type, in which the oxidized bacteriochlorophyll dimer results in an EPR spectrum centered at $g = 2.0025$. The calculated integrated amplitudes of the signals revealed almost the same amount of signal being formed for all mutants, with the amplitudes

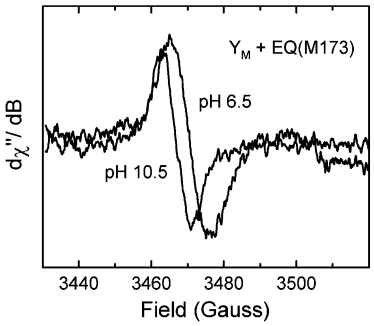

FIGURE 6: Normalized light-minus-dark X-band EPR spectra of reaction centers at pH 6.5 and 10.5 from the Y_M + EQ(M173) mutant. At pH 6.5 the calculated *g* value is 2.0022 ± 0.0005, and at pH 10.5 the *g* value is 2.0044 ± 0.0005. Each spectrum is the average from 100 light and dark scans measured at room temperature.

being 5% ± 1% of the wild-type oxidized bacteriochlorophyll dimer signal.

The EPR spectra of the mutants were found to have a pronounced pH dependence (Figure 6). For example, at pH 6.5, a single derivative with a *g* value of 2.0022 was observed in the spectrum of the Y_M + EQ(M173) mutant, whereas at pH 8 and 10.5, the derivative signals have *g* values of 2.0042 and 2.0044, respectively. It is likely that under the illumination conditions used for these EPR spectra, the signal attributed to the tyrosyl radical preferentially accumulates due to a difference in the lifetime of the tyrosyl radical compared to that of the oxidized dimer.

DISCUSSION

Reaction centers from mutants containing a tyrosine residue near a highly oxidizing dimer were found to exhibit characteristics that are generally similar to those of wild type at low pH but are significantly different at high pH. The new spectral features are identified as arising from an oxidized tyrosine as discussed previously (*6*) and below. The oxidation of the tyrosine is due to an electron-transfer process that is highly pH-dependent, indicating that the protonation state of specific residues in the protein environment is critical in establishing the properties of the tyrosine radical. The implications of coupling between proton and electron transfer for the tyrosine radicals in this system can be compared to the proton-dependent properties of amino acid radicals in other proteins.

Identification of Tyrosine as the Secondary Electron Donor in the Mutants. The optical spectra show the presence of a new state that is coupled to the loss of the oxidized dimer (Figure 2). The formation of the new state is highly pH-dependent and fully reversible. At high pH, bleaching of the 865 nm band is not observed, but the electrochromic shift of the 760 nm band is present, indicating the presence of a semiquinone and the lack of the oxidized dimer. These features can be explained by the light-induced formation of a charge-separated state involving the oxidized dimer and reduced quinone followed by reduction of the oxidized dimer by a secondary electron donor. When the tyrosine at M164 is not present in the highly oxidizing mutants, none of these new spectral features are present (*6*). Thus, the new state is associated with the presence of the tyrosine at residue M164, and the most probable conclusion is that this residue serves as a secondary electron donor to the dimer.

The EPR spectra corroborate the presence of a tyrosyl radical in the mutants. The signals at high pH have a *g* value characteristic of tyrosyl radicals and do not arise from an uncoupled reduced quinone, which would have a similar *g* value (*6*). The EPR signals undergo a pH dependence as do the optical spectra, indicating that the EPR and optical signals arise from the same pH-dependent states. The spectra are fully reversible with the removal of light, demonstrating that they arise from a well-defined electron-transfer process rather than a nonspecific degradation process.

In most proteins containing tyrosyl radicals, the EPR signals show characteristic hyperfine couplings (*5*). For the mutants presented here, the hyperfine couplings may be present but not evident in the spectra due to the limited signal-to-noise ratio of the EPR signals. This low signal-to-noise ratio arises from both the low quantum yield of these mutants and limitations arising from the measurement at room temperature of the EPR signals. Alternatively, because the hyperfine coupling is sensitive to the geometry of the tyrosyl and so has a strong angular dependence on orientation (*9*), the lack of observed hyperfine coupling may arise from a disorder in the orientation of the tyrosyl. Similar signals have also been seen for amino acid radicals generated in some photosystem II mutants (*10*−*12*), rhenium-modified azurin (*6*), and small peptides (*13*).

Modeling the pH Dependence of Spectral Features. The formation of the tyrosyl signal, as identified by the presence of a negative absorption change at 420 nm, was correlated with diminishing of the extent of bleaching of the oxidized dimer (Figure 3). This correlation is found for all of the mutants; however, differences among the mutants are evident in the pK_a determined for this dependence. Since the same tyrosine residue at M164 is the proposed secondary donor to the oxidized dimer for all of these mutants, the differences in the pH dependencies must arise from altered interactions between the tyrosine and the surrounding protein. A neutral tyrosyl radical is much more stable than a charged tyrosine, so a protonated tyrosine is expected to release the phenolic proton upon oxidation (*14*). In this case, a suitable proton acceptor near the tyrosine is required to accept the phenolic proton. Alternatively, at high pH, the tyrosine itself could be deprotonated, negating the requirement for a proton acceptor. Thus, the observed pK_a associated with the formation of the tyrosyl radical could reflect the protonation state of either a proton acceptor or the tyrosine.

For the Y_M mutant, the extent of formation of the tyrosyl signal can be fitted by a Henderson−Hasselbalch dependence with a pK_a of 6.9. This pH dependence probably reflects the protonation state of His M193 (*6*). In this model, at pH values significantly lower than the pK_a of 6.9, His M193 would be protonated and could not accept the phenolic proton from the tyrosine, resulting in a limited stability of the tyrosyl radical. At high pH values, His M193 would be deprotonated and could serve as a proton acceptor. In the Y_M mutant, measurable amounts of the tyrosyl signal remain at pH 6, where a proton acceptor with a pK_a of 6.9 would no longer be effective. This residual signal could be attributed to a second proton acceptor, probably Glu M173, which would be expected to have a low pK_a and remain functional at pH 6. Thus the behavior of the Y_M mutant can be explained by His M193 serving as the major proton acceptor with a pK_a of 6.9 and Glu M173 contributing to a lesser extent.

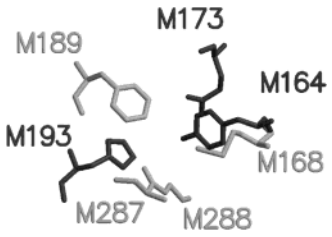

FIGURE 7: Structural representation of the environment of the tyrosyl radical at M164 in the Y_M mutant based upon the three-dimensional structure of wild-type reaction centers. The Tyr at M164 is proposed to make a hydrogen bond with His M193 and to donate a proton to either His M193 or Glu M173 upon oxidation. The surrounding protein forms a hydrophobic pocket consisting of amino acid residues Met M168, Phe M189, Ser M287, and Gly M288.

The substitution of Gln for His M193 in the Y_M + HQ-(M193) mutant should have the effect of removing the major proton acceptor. In this mutant, the extent of formation of the tyrosyl is limited, and the pH dependence yields a very high pK_a of approximately 10. Because the substitution of Gln at M193 results in the loss of the proton acceptor, only at high pH when the tyrosine is deprotonated would there be a neutral radical after oxidation. Hence, the observed pK_a of the pH dependence in this mutant probably directly reflects the pK_a of Tyr M164. This pK_a is similar to the pK_a values of 9−10 for tyrosine in solution.

Substitution of the putative proton acceptor His M193 with alternate proton acceptors such as Tyr in the Y_M + HY-(M193) mutant and Glu in the Y_M + HE(M193) mutant should have the effect of shifting the pK_a value observed for the formation of the tyrosyl. Upon substitution of Tyr for His at M193, the observed increase in the pK_a of the tyrosyl formation from 6.9 to 8.9 is consistent with the intrinsically higher pK_a of tyrosine compared to histidine. This behavior is similar to that observed in mutants in which a tyrosyl radical is formed at L135, the residue symmetry-related to M164, for which Tyr L164 is found in the corresponding position to M193 (*6*). The substitution of Glu at M193 also results in the pH dependence of the tyrosyl formation having a pK_a of 8.9, although this is much higher than the pK_a of 4−5 observed for Glu in solution. This mutation places two glutamic acid residues in close proximity, and the resulting electrostatic interactions could alter the pK_a of Glu M193. Large shifts in the pK_a values of glutamic acid residues have been demonstrated for other cases, such as Glu L212 near the secondary quinone (*15*).

In each of the mutants, Y_M, Y_M + HE(M193), Y_M + HY-(M193), and Y_M + HQ(M193), a measurable formation of the tyrosyl remains at pH 6−7 (Figure 4). This residual signal at low pH was attributed to another nearby amino acid residue serving as proton acceptor, with Glu M173 considered to be a likely candidate (Figure 7). Replacement of Glu M173 with Gln in the Y_M + EQ(M173) mutant results in a value near zero for the tyrosyl signal at low pH values (Figure 4), consistent with this model. This mutation also results in a shift of the observed pK_a, possibly because the protonated and positively charged form of His M193 is no longer stabilized by a negative charge from Glu M173.

The redox-active tyrosine at M164 and the nearby proton acceptors are located in a relatively hydrophobic region near the periplasmic surface of the protein. In wild type, Arg M164 primarily forms a salt bridge with Glu M173 but also has a weaker interaction with His M193. Other residues near M164 include Phe M189, Met M168, Ser M287, and Gly M288 (Figure 7). Based upon the similarity of the spectral characteristics and the sizes of Tyr and Arg, the replacement Arg M164 to Tyr most likely does not significantly alter the structure, and the protein environment surrounding M164 should be similar to that in wild type. Assuming that the backbone does not change in the mutant, the most likely positioning of the Tyr places the phenolic proton in hydrogen-bonding position to the Nϵ of His M193. Glu M173 would also be within 3.5 Å of Tyr M164, although the orientation makes it unlikely to form a hydrogen bond. Thus, His M193 and Glu M173 would be well positioned to serve as proton acceptors as described above.

Modeling of the orientation of Tyr M164 also allows an alternate structural model in which Ser M287 interacts with Tyr M164 and His M193. This configuration may become active if the Tyr M164/His M193/Glu M173 group becomes disrupted due to mutations. It is possible that the pK_a observed in some of the mutants reflects Ser M287 deprotonation being a limiting step in the proton acceptor network. Although Ser is usually unwilling to accept a proton, it has been known to participate in proton transfer in other proteins, such as α-chymotrypsin, where serine plays a major role in proton transfer and formation of the catalytic triad (*16*). In addition, water molecules in the vicinity of Tyr M164 may participate, and involvement of backbone carbonyls in proton transfer has also been shown to occur in several systems, including phenol hydroxylase and *p*-hydroxylbenzoate hydroxylase (*17*).

Implications for Amino Acid Radicals in Other Proteins. The results show that it is possible to correlate the properties of tyrosyl radicals in the bacterial reaction center with the molecular properties of nearby proton acceptors. Proton acceptors have been demonstrated to play critical roles in other proteins having amino acid radicals. For example, in class I ribonucleotide reductases, the coupled transfer of a proton and an electron has been proposed to occur in diverging pathways, with the transfer of the proton occurring via flexible charged neighboring residues (*5*). The ability to generate the tyrosyl radical with light in the bacterial reaction center makes it a useful system for probing the role of proton acceptors in regulating the properties of tyrosyl radicals in other proteins, in particular, in the evolutionarily related photosystem II. Photosystem II contains a redox-active tyrosine Y_Z that serves a critical role as an intermediate electron acceptor between the oxidized chlorophyll donor and the manganese complex (see ref *18* for a review).

The amino acid residues surrounding Y_Z have been modeled as actively participating in the water oxidation process (*19*−*22*). Two amino acid residues, Glu 189 and His 190 of the D1 polypeptide, have been proposed to play key roles in the coupling of the electron-transfer processes with the transfer of the phenolic proton of Y_Z, identified as residue Tyr 161, and Asp 170 serves as a Mn ligand (see refs *23* and *24* for reviews). The interactions involving the nearby amino acid residues and Y_Z are difficult to probe because Y_Z serves as a short-lived transient acceptor. In particular, the pH dependencies derived from spectroscopic measurements have been modeled with a wide range of pK_a values, from 7 to 9 in wild type and from 8 to 10 in complexes with

mutations at His 190 *(22*−*26)*. Based upon a sequence comparison, Tyr 161, Asp 170, and His 190 of the D1 subunit in photosystem II are found in the positions corresponding to the triad of residues Tyr M164, Glu M173, and His M193, respectively, which appear to be required for the Tyr M164 radical in the reaction center to have a pK_a of 7. With this assumption, our results are consistent with the properties of Y_Z having a pK_a of approximately 7 for the wild type that increases to a pK_a of approximately 10 in mutants in which the proton acceptor at His 190 is removed. In photosystem II, one key outstanding question concerns the fate of the phenolic proton of Y_Z. In the hydrogen abstraction models, the proton transfers into the lumen, but it has also been argued that the proton does not leave the local environment of Y_Z (*14*, *27*). A substantial increase in proton release is observed for the Y_M mutant relative to wild type (*28*). The release of the proton may be facilitated by nearby residues, similar to what has been argued for photosystem II *(23*, *24)*.

In conclusion, these results provide a biochemical model for the interpretation of amino acid radicals in more complex systems. The importance of the local environment in the formation of the tyrosyl radical points toward the involvement of hydrogen-bonding networks.

ACKNOWLEDGMENT

We thank M. Thielges for cell growth.

REFERENCES

1. Blankenship, R. E., Madigan, M. T., and Bauer, C. E., Eds. (1995) *Anoxygenic Photosynthetic Bacteria*, Kluwer Academic Publishers, Dordrecht, The Netherlands.
2. Allen, J. P., and Williams, J. C. (1998) *FEBS Lett. 438*, 5−9.
3. Sjöberg, B. M., Reichard, P., Gräslund, A., and Ehrenberg, A. (1977) *J. Biol. Chem. 252*, 536−541.
4. Stubbe, J., and van der Donk, W. A. (1998) *Chem. Rev. 98*, 705−762.
5. Kálmán, L., LoBrutto, R., Allen, J. P., and Williams, J. C. (1999) *Nature 402*, 696−699.
6. Di Bilio, A. J., Crane, B. R., Whebi, W. A., Kiser, C. N., Abu-Omar, M. M., Carlos, R. M, Richards, J. H., Winkler, J. R., and Gray, H. B. (2001) *J. Am. Chem Soc. 123*, 3181−3182.
7. Lin, X., Murchison, H. A., Nagarajan, V., Parson, W. W., Allen, J. P., and Williams, J. C. (1994) *Proc. Natl. Acad. Sci. U.S.A. 91*, 10265−10269.
8. Williams, J. C., Alden, R. G., Murchison, H. A., Peloquin, J. M., Woodbury, N. W., and Allen, J. P. (1992) *Biochemistry 31*, 11029−11037.
9. Hoganson, C. W., Sahlin, M., Sjöberg, B. M., and Babcock, G. T. (1996) *J. Am. Chem. Soc. 118*, 4672−4679.
10. Tommos, C., Davidsson, L., Svensson, B., Madsen C., Vermaas, W., and Styring, S. (1993) *Biochemistry 32*, 5436−5441.
11. Un, S., Tang, X. S., and Diner, B. A. (1996) *Biochemistry 35*, 679−684.
12. Manna, P., LoBrutto, R., Eijckelhoff, C., Dekker, J. P., and Vermaas, W. (1998) *Eur. J. Biochem. 251*, 142−154.
13. Ayala, I., Range, K., York, D., and Barry, B. A. (2002) *J. Am. Chem. Soc. 124*, 5496−5505.
14. Tommos, C., and Babcock, G. T. (2000) *Biochim. Biophys. Acta 1458*, 199−219.
15. Okamura, M. Y., Paddock, M. L., Graige, M. S., and Feher, G. (2000) *Biochim. Biophys. Acta 1458*, 148−163.
16. Wells, J. A., and Estell, D. A. (1988) *Nature 332*, 564−568.
17. Ridder, L., Mulholland, A. J., Rietjens, I. M. C. M., and Vervoort, J. (2000) *J. Am. Chem. Soc. 122*, 8728−8738.
18. Ort, D. R., and Yocum, C. F., Eds. (1996) *Oxygenic Photosynthesis*: *The Light Reactions*, Kluwer Academic Publishers, Dordrecht, The Netherlands.
19. Hoganson, C. W., and Babcock, G. T. (1997) *Science 277*, 1953−1956.
20. Gilchrist, M. L., Jr., Ball, J. A., Randall, D. W., and Britt, R. D. (1995) *Proc. Natl. Acad. Sci. U.S.A.* 92, 9545−9549.
21. Tang, X. S., Randall, D. W., Force, D. A., Diner, B. A., and Britt, R. D. (1996) *J. Am. Chem. Soc. 118*, 7638−7639.
22. Mamedov, F., Sayre, R. T., and Styring, S. (1998) *Biochemistry 37*, 14245−14256.
23. Diner, B. A. (2001) *Biochim. Biophys. Acta 1503*, 147−163.
24. Debus, R. J. (2001) *Biochim. Biophys. Acta 1503*, 164−186.
25. Hays, A.-M. A., Vassiliev, I. R., Goldbeck, J. H., and Debus, R. J. (1998) *Biochemistry 37*, 11352−11365.
26. Hays, A.-M. A., Vassiliev, I. R., Goldbeck, J. H., and Debus, R. J. (1999) *Biochemistry 38*, 11851−11865.
27. Haumann, M., and Junge, W. (1999) *Biochim. Biophys. Acta 1411*, 86−91.
28. Kálmán, L., Williams, J. C., and Allen, J. P. (2002) *FEBS Lett.* (submitted for publication).

BI0264566